Search for 2β decay of cerium isotopes with $CeCl_3$ scintillator

2011 J. Phys. G: Nucl. Part. Phys. 38 015103

(http://iopscience.iop.org/0954-3899/38/1/015103)

J. Phys. G: Nucl. Part. Phys. **38** (2011) 015103 (15pp) doi:10.1088/0954-3899/38/1/015103

Search for 2β decay of cerium isotopes with $CeCl_3$ scintillator

P Belli[1], R Bernabei[1,2,7], F Cappella[3,4], R Cerulli[5], F A Danevich[6], A d'Angelo[3,4], A Di Marco[5], A Incicchitti[3], F Nozzoli[1,2] and V I Tretyak[6]

[1] INFN, Sezione di Roma Tor Vergata, I-00133 Rome, Italy
[2] Dipartimento di Fisica, Università di Roma 'Tor Vergata', I-00133 Rome, Italy
[3] INFN, Sezione di Roma, I-00185 Rome, Italy
[4] Dipartimento di Fisica, Università di Roma 'La Sapienza', I-00185 Rome, Italy
[5] INFN, Laboratori Nazionali del Gran Sasso, 67010 Assergi (AQ), Italy
[6] Institute for Nuclear Research, MSP 03680 Kyiv, Ukraine

E-mail: rita.bernabei@roma2.infn.it

Received 16 September 2010
Published 9 December 2010
Online at stacks.iop.org/JPhysG/38/015103

Abstract

Double beta processes in ^{136}Ce, ^{138}Ce and ^{142}Ce have been searched for by exploiting the active source approach with the help of a 6.9 g $CeCl_3$ crystal as a scintillator for the first time at the Gran Sasso National Laboratory (LNGS) of the INFN (Italy). The total measurement time is 1638 h; even such a small exposure has allowed the achievement of some improved half-life limits on 2β decay processes in these isotopes at the level of 10^{16}–10^{18} yr. In particular (90% C.L.): $T_{1/2}^{0\nu\varepsilon\beta^+}(^{136}\mathrm{Ce}) \geqslant 8.8 \times 10^{16}$ yr, $T_{1/2}^{2\nu\varepsilon\beta^+}(^{136}\mathrm{Ce}) \geqslant 2.4 \times 10^{16}$ yr, $T_{1/2}^{2\nu 2K}(^{136}\mathrm{Ce}) \geqslant 3.2 \times 10^{16}$ yr, $T_{1/2}^{2\nu 2K}(^{138}\mathrm{Ce}) \geqslant 4.4 \times 10^{16}$ yr, and $T_{1/2}^{2\nu 2\beta^-}(^{142}\mathrm{Ce}) \geqslant 1.4 \times 10^{18}$ yr. Possible future perspectives are also briefly addressed.

(Some figures in this article are in colour only in the electronic version)

1. Introduction

The neutrinoless (0ν) double beta (2β) decay of atomic nuclei $(A, Z) \rightarrow (A, Z \pm 2) + 2e^{\mp}$ is forbidden in the Standard Model (SM) since it violates the lepton number by two units [1]; however, it is predicted in many SM extensions. The double beta decay experiments are considered the best way to determine an absolute scale of the neutrino mass, to probe the nature of the neutrino, to establish the neutrino mass hierarchy, to search for the existence of right-handed admixtures in the weak interaction, and to test some other effects beyond the SM. During the last two decades the experimental sensitivity to the $0\nu 2\beta^-$ decay mode reached levels up to 10^{23}–10^{25} yr [1].

[7] Author to whom any correspondence should be addressed.

Table 1. Potentially 2β active nuclides present in $CeCl_3$ crystals.

Transition	Energy release (keV) [12]	Isotopic abundance (%) [13]	Decay channels	Number of nuclei in 100 g of $CeCl_3$ crystal
$^{136}Ce \rightarrow {}^{136}Ba$	2419(13)	0.185(0.002)	2ε, $\varepsilon\beta^+$, $2\beta^+$	4.52×10^{20}
$^{138}Ce \rightarrow {}^{138}Ba$	693(10)	0.251(0.002)	2ε	6.13×10^{20}
$^{142}Ce \rightarrow {}^{142}Nd$	1416.7(2.1)	11.114(0.051)	$2\beta^-$	2.72×10^{22}

In the SM the two-neutrino (2ν) double beta decay is an allowed rare process; to date it is the rarest decay observed in direct laboratory experiments. It was detected only for ten nuclides, and the corresponding half-lives are in the range of 10^{18}–10^{24} yr [2, 3].

So far the experimental investigations in this field have been mainly focused on the $2\beta^-$ decays, while the results for double positron decay ($2\beta^+$), electron capture with positron emission ($\varepsilon\beta^+$), and capture of two electrons from the atomic shells (2ε) are much more modest (the most sensitive experiments gave limits on the 2ε, $\varepsilon\beta^+$ and $2\beta^+$ processes at the level of 10^{17}–10^{21} yr [2, 4, 5]). This is due to: (i) the lower energy releases in the 2ε, $\varepsilon\beta^+$ and $2\beta^+$ processes with respect to those in the $2\beta^-$ decay (which imply lower probabilities for the processes and make the background suppression difficult); (ii) the natural abundances of $2\beta^+$ isotopes (typically lower than 1% with only a few exceptions). Nevertheless, efforts are in progress in this direction since the studies of the neutrinoless 2ε and $\varepsilon\beta^+$ decays could help to investigate the contribution of right-handed admixtures in weak interaction to the neutrinoless $2\beta^-$ decay [6].

An interesting case is cerium; in fact, it offers three double beta decaying isotopes: ^{136}Ce, ^{138}Ce and ^{142}Ce (see table 1), and the recent development of new scintillating materials containing Ce also allows the exploitation of the efficient 'source = detector' approach. In particular, ^{136}Ce is a very interesting isotope since the high energy release allows the $2\beta^+$ decay mode, which is energetically possible only for six candidate nuclei [2]. Moreover, some resonant neutrinoless 2ε captures in ^{136}Ce to the excited states of ^{136}Ba are also energetically allowed (see e.g. [7]).

Up to now, the possible 2β decays of Ce isotopes were searched for only in four experiments: three of them exploited the active source approach with CeF_3 [8, 9] and GSO(Ce) crystals [10], and one the passive source approach with HPGe detector using the same $CeCl_3$ as in this work [11]. The processes were not detected and only limits on half-lives were set; for ^{136}Ce and ^{138}Ce they were in the range of 10^{15}–10^{17} yr; for ^{142}Ce they were in the range of 10^{17}–10^{19} yr.

In this paper we report the results obtained in the investigation of the 2β processes in Ce isotopes using for the first time the $CeCl_3$ crystal as a scintillator to realize the 'source = detector' approach.

Table 1 summarizes the main information about the possible 2β decays in the $CeCl_3$ crystal.

2. Experimental set-up and measurements

2.1. $CeCl_3$ crystal scintillator

In recent years scintillating materials containing cerium have attracted much attention in the developments of new fast scintillators with high density, large light yield, perfect linearity

and good energy resolution for applications in fundamental and applied nuclear and particle physics, and in several other fields. In fact—due to the electric dipole allowed 5d–4f transitions in the atomic shell—the Ce^{3+} ions yield fast (10–100 ns) scintillation in the 300–500 nm wavelength range [14, 15]. Scintillating crystals such as CeF_3, $CeBr_3$ and $CeCl_3$, where Ce is not a dopant but a main constituent, were also studied.

In particular, the detector used in the present measurements is a cylindrical $\oslash 13 \times 13$ mm^2 $CeCl_3$ crystal (6.9 g mass), housed—because of its hygroscopicity—in a combined plastic and copper container ($\oslash 16 \times 20$ mm^2 external size). Previous measurements were carried out on the detector radiopurity by using a HPGe detector deep underground at LNGS [11], and main scintillation features were studied in [16].

The present data taking has been performed by equipping the crystal with a $\oslash 7.6 \times 10$ cm^2 Tetrasil-B light guide to further reduce the contribution of the used 3″ low background photomultiplier (PMT) to the background. The detector has been installed deep underground ($\simeq$3600 m w.e. (metres water equivalent)) in the low background DAMA/R&D set-up [5, 17] at LNGS. It was surrounded by Cu bricks and sealed in a low radioactive air-tight Cu box continuously flushed with high purity nitrogen gas (stored deeply underground for a long time) to avoid the presence of residual environmental radon. The copper box was surrounded by a passive shield made of 10 cm of high purity Cu, 15 cm of low radioactive lead, 1.5 mm of cadmium and 4/10 cm polyethylene/paraffin to reduce the external background. The whole shield has been closed inside a plexiglas box, also continuously flushed by high purity nitrogen gas.

The signals from the PMT have been recorded—over a time window of 4000 ns and a sampling time of 1 GSample/s—by an 8 bit DC270 Acqiris transient digitizer (TD).

2.2. Calibration

The energy scale and the energy resolution of the $CeCl_3$ scintillator detector have been measured by using the following γ sources: (i) ^{133}Ba (81 and 356 keV); (ii) ^{22}Na (511 and 1275 keV); (iii) ^{137}Cs (662 keV); (iv) ^{60}Co (1173 and 1333 keV); see figure 1. The linearity of the energy calibration is shown in figure 2.

The dependence of the energy resolution of the $CeCl_3$ detector on the energy can be fitted by the function $\sigma_\gamma/E_\gamma = a + b/\sqrt{E_\gamma}$, where E_γ is the energy of the γ quanta in keV; in particular, for the present assembly: $\sigma_\gamma/E_\gamma = 0.0121 + 0.237/\sqrt{E_\gamma}$.

2.3. Pulse shape discrimination capability

The pulse shape discrimination (PSD) capability between α and $\gamma(\beta)$ particles has been investigated in [16] with the crystal directly coupled to the PMT; the pulses, recorded by a 2.5 GSample/s TD over a time window of 500 ns, were analysed and good discrimination capability was found for the $CeCl_3$ crystal.

In this work the possibility of applying the PSD to the production data collected with the $CeCl_3$ crystal in the present assembly (light guide and a 1 GSample/s TD) has been investigated. In particular, we use the optimal digital filter method [18]. For each signal $f(t)$, the numerical characteristic of its shape (shape indicator, SI) was defined as $\mathrm{SI} = \sum f(t_k) \times P(t_k) / \sum f(t_k)$, where the sum is over the time channels k, starting from the origin of signal and averaging up to 70 ns. The $f(t_k)$ is the digitized amplitude (at the time t_k) of a given signal. The weight function $P(t)$ was defined as $P(t) = \{f_\alpha(t) - f_\gamma(t)\}/\{f_\alpha(t) + f_\gamma(t)\}$, where $f_\alpha(t)$ and $f_\gamma(t)$ are the reference pulse shapes for α particles and γ quanta, respectively, obtained by summing up shapes of a few thousand γ or α events. To build the γ reference pulse we considered the data collected with the ^{22}Na and ^{60}Co sources, while for the α we considered the data

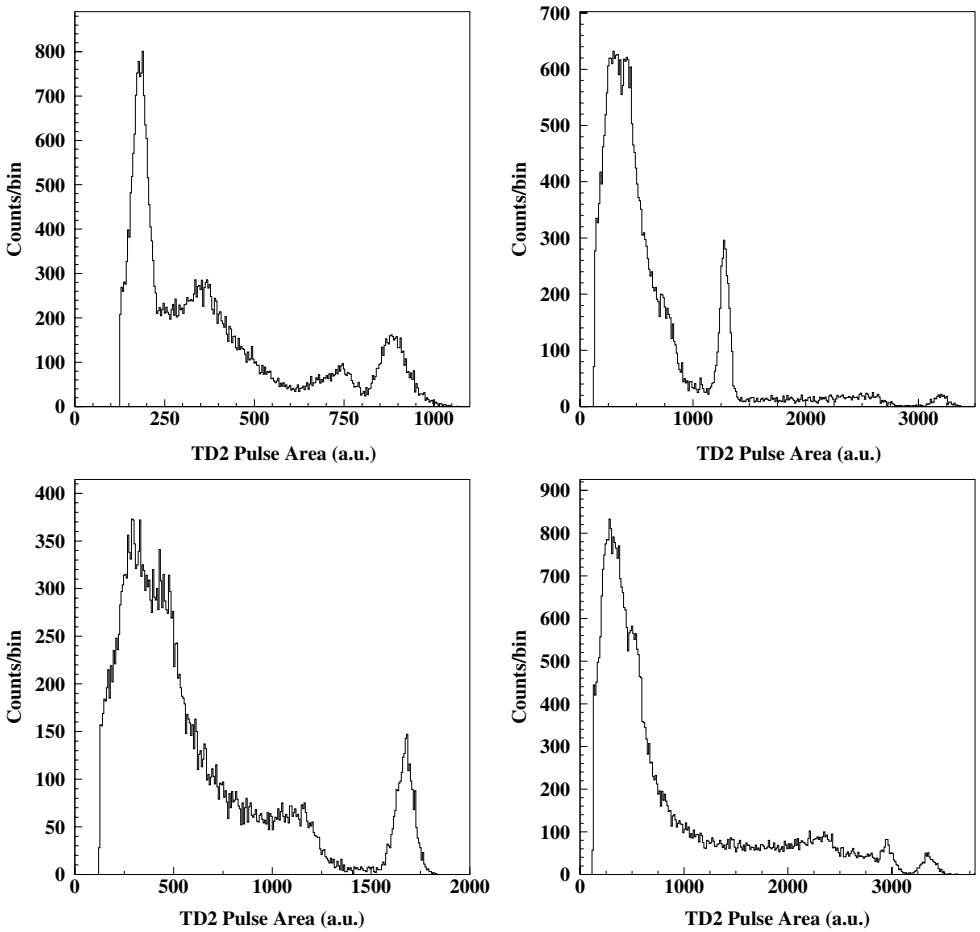

Figure 1. Energy distributions measured by the $CeCl_3$ detector in the assembly with light guide when using the following γ sources: (top left) ^{133}Ba; (top right) ^{22}Na; (bottom left) ^{137}Cs; (bottom right) ^{60}Co. See the text.

collected in the production runs in the 1.5–2.3 MeV energy range[8], where the α contribution to the experimental energy distribution is dominant (see later). The distributions of the shape indicator for the two classes of events (energies above 1 MeV in γ scale) are depicted in figure 3; they are well described by Gaussian functions. Although there is still a statistical separation between the two populations in the present assembly of the $CeCl_3$ crystal, it is poorer than in [16]; this can be ascribed to the presence of the light guide, which reduces the far UV component of the scintillation light, and to the smaller sampling frequency. Thus, cautiously in the following analyses we will not profit by it.

2.4. Internal contaminations of the $CeCl_3$

In [16] the residual contaminations in the $CeCl_3$ crystal were investigated and discussed in detail; moreover, the activity of the $CeCl_3$ detector (including housing) was also previously

[8] The α energies are given in terms of calibrations with γ sources, that is in MeV electron equivalent. See also later in the figures.

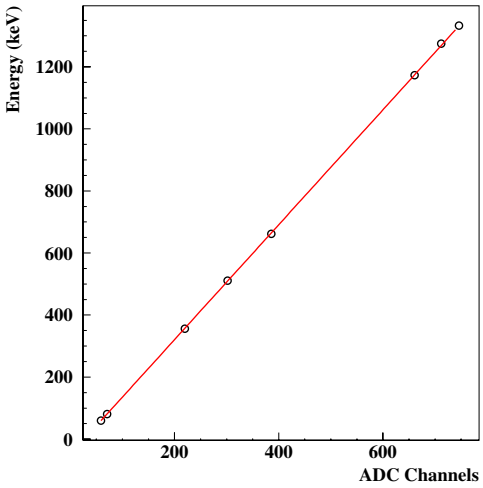

Figure 2. Linearity of the energy response of the $CeCl_3$ scintillator as measured with the γ sources.

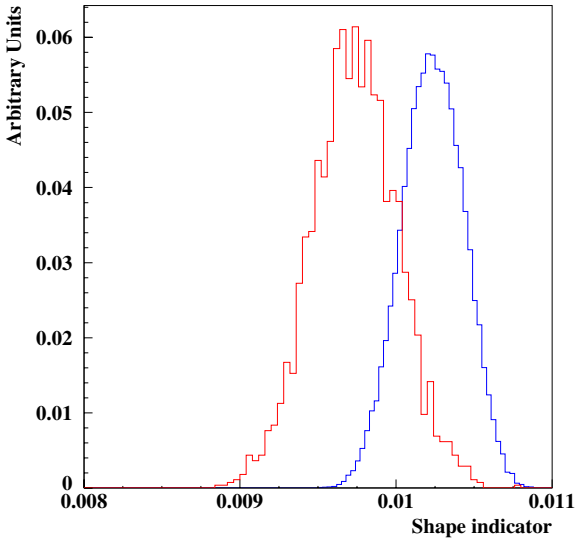

Figure 3. Shape indicator distributions of the events collected above 1 MeV: α particles (red, lower SI), γ particles (blue, higher SI).

investigated in [11] on the basis of HPGe γ spectrometry. The present larger exposure and the used approach improve such an investigation in some aspects.

The energy distribution, measured deep underground in the present low background set-up during the 1638 h of data taking, is shown in figure 4.

The measured background has similar behaviour as in [16] and is dominated by the internal residual contaminants; in particular, the events below $\simeq$1400 keV are mainly due to the radioactive decays of ^{138}La and to the β decays of radioactive isotopes in the ^{235}U chain to which the α particles observed above $\simeq$1400 keV belong. This has also allowed the

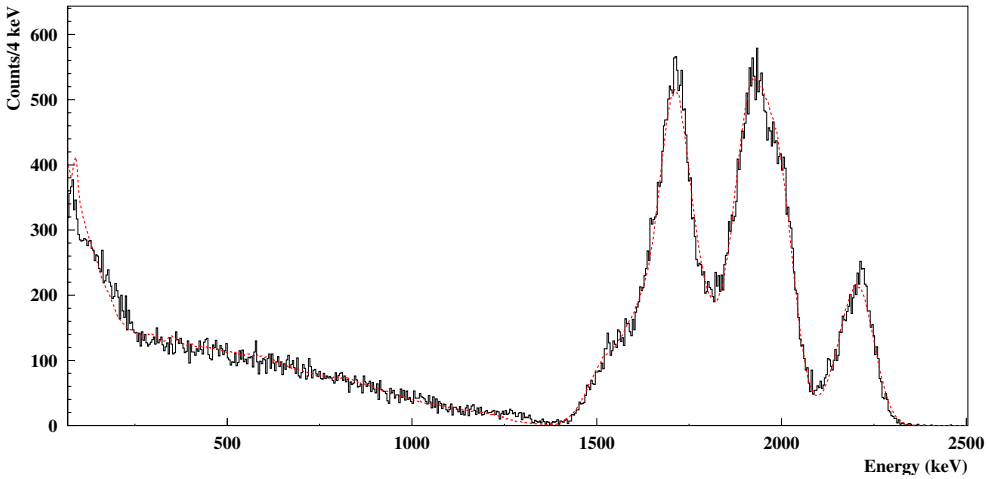

Figure 4. Energy distribution measured deep underground during 1638 h live time inside the multi-component low background passive shield; the superimposed curve is the overall background fit estimated as in figures 9 and 11 of [16], where also the main components were shown. The background fit is in good agreement with the experimental data with the exception just of the lowest energy bins; for this reason in the determination of the results on the double electron capture decay channels of ^{136}Ce and ^{138}Ce isotopes this fit has not been applied.

Table 2. Radioactive contamination of the $CeCl_3$ crystal. The upper limits (90% C.L.) arise from the analysis of the Bi–Po events. The chains have been considered in equilibrium.

Decay chain	Nuclide	Activity (mBq kg^{-1})	Contamination from the chain
^{232}Th	^{228}Th	<0.16	<40 ppt
^{235}U	^{227}Ac	=284(2)	=3.52(0.03) ppb
^{238}U	^{226}Ra	<11	<0.9 ppb
	^{138}La	=862(31)	=948(35) ppb

determination of the relative light yield for α particles as compared with that for γ quanta—the so-called α/β ratio[9]: $\alpha/\beta = 0.070 + 0.050 \times E_\alpha - 0.0026 \times E_\alpha^2$, where E_α is the energy of the α particles in MeV (E_α between 5.5 and 7.5 MeV).

In particular, the energy distribution of figure 4 has been analysed in order to more precisely determine the ^{235}U and ^{138}La content in the crystal, following the same procedures as in [16] where the energy spectrum was compared with Monte Carlo expectations; the values obtained here are given in table 2. The contents of ^{238}U and of ^{232}Th have been determined by analysing time correlated events in the TD time window (4000 ns) as described in the following.

During the present live time 14 double pulse events have been identified; two examples of them have already been shown in figure 7 of [16]. These double pulse events cannot be ascribed to random coincidence; in fact, considering the mean rate measured above the energy

[9] The α/β ratio is defined as the ratio of α peak position in the energy scale measured with γ sources to the energy of α particles (E_α). Because γ quanta interact with the detector by β particles, we use the more convenient term 'α/β' ratio.

threshold of $\simeq$ 50 keV and the effective TD time window ($\simeq$ 3650 ns), the expected number of random coincidences during the present data taking is 8.3×10^{-5}.

The measured events can mainly be ascribed to α–α time correlated events produced by α decay of ^{219}Rn into ^{215}Po followed by ^{215}Po α decay ($T_{1/2}$ ~1.781 ms) into ^{211}Pb (isotopes of the ^{235}U chain). In particular, the first pulse in each event can be due to the ^{219}Rn α decay (79.4% α of 6.819 MeV, 12.9% α of 6.553 MeV and 7.5% α of 6.425 MeV), while the second one can be due to the ^{215}Po α decay ($\simeq$ 100% α of 7.386 MeV). Moreover, the number of the measured time correlated events (14) is in agreement with the expected number of α–α events in the effective TD time window: 16 α–α events, which can be derived from the ^{235}U measured contamination in the detector (see table 2). Thus, upper limits on Bi–Po events can be set.

A Bi–Po event from ^{232}Th chain is given by the β decay of ^{212}Bi into ^{212}Po followed by the ^{212}Po α decay ($T_{1/2} = 299(2)$ ns; 100% α of 8.785 MeV), while a Bi–Po event from ^{238}U chain is given by the β decay of ^{214}Bi into ^{214}Po followed by the ^{214}Po α decay ($T_{1/2} =$ 164.3(2.0) μs; $\simeq$ 100% α of 7.687 MeV). The detection efficiency in the effective TD time window is $\simeq$100% for Bi–Po events of the ^{232}Th chain and 1.5% for those of the ^{238}U chain.

Considering the expected α–α events from the ^{235}U residual contamination as background with respect to the Bi–Po events, the Bayesian approach [19] allows the estimation of the upper limit on the number of Bi–Po events: 6.61 (90% C.L.) from both ^{238}U and ^{232}Th chains. Thus, the activities: $a_{^{212}\mathrm{Bi}-^{212}\mathrm{Po}} \leqslant 0.16$ mBq kg^{-1} and $a_{^{214}\mathrm{Bi}-^{214}\mathrm{Po}} \leqslant 11$ mBq kg^{-1} (90% C.L.) are derived; then, considering the chains in equilibrium, the upper limits on the ^{232}Th and on the ^{238}U contaminations are achieved (see table 2).

The obtained limits and values are compatible and more precise than those of [11, 16] with the only exception of the ^{238}U residual contamination, which was significantly higher in the HPGe measurements [11]; this can be ascribed—as already discussed also in [16]—to a few mBq ^{238}U residual contamination in the housing materials (copper, optical window, etc) which are of commercial quality.

3. The investigation of the 2β decay modes

As discussed in the following, there are no clear peculiarities in the energy distribution measured by the $CeCl_3$ detector, which could be interpreted as double beta decay of cerium isotopes. Therefore, only lower half-life limits can be set according to the formula

$$\lim T_{1/2} = N \cdot \eta \cdot t \cdot \ln 2 / \lim S,$$

where N is the number of potentially 2β unstable nuclei, η is the detection efficiency, t is the measuring time, and $\lim S$ is the number of events of the effect searched for which can be excluded at a given confidence level. The values of η in the considered energy interval, of S/η (see later) and of $\lim S$ for each considered decay mode are summarized in table 3.

The response functions of the $CeCl_3$ detector for the 2β processes have been simulated with the help of the EGSnrc code [20]; the initial kinematics of the particles emitted in the decays has been generated with the DECAY0 event generator [21]. A similar procedure has been used to evaluate the background contribution from the measured residual contaminations.

Preliminarily the experimental sensitivity to each considered double beta decay mode is estimated by using the so-called 1σ approach where the excluded number of the events due to the effect searched for is estimated simply as the square root of the number of background counts in the chosen energy window; if the expected signal is a peak the considered energy interval is $\pm 1\ \sigma$ around the expected signal peak. Notwithstanding its simplicity, this method

Table 3. Values of the interesting quantities for the calculation of the $T_{1/2}$ limits on the various decay channels (see later). The overall uncertainty on each η value does not exceed 5%.

Transition	Decay channel	Decay mode	Energy range (keV)	Efficiency η	S/η	$S_{\rm lim}/\eta$ 90%(68%) C.L.
^{136}Ce $\rightarrow$ ^{136}Ba	$2\beta^+$	0ν	320–436	48%	$-(99 \pm 81)$	55(16)
		2ν	596–840	17%	$-(197 \pm 393)$	465(221)
	$\epsilon\beta^+$	0ν	1328–1504	54%	$-(53 \pm 55)$	46(16)
		2ν	200–1000	86%	$-(102 \pm 160)$	171(75)
	$2K$	0ν	56–92	79%	(58 ± 48)	137(106)
		2ν	56–92	87%	(53 ± 44)	125(97)
^{138}Ce $\rightarrow$ ^{138}Ba	$2K$	0ν	56–92	73%	(64 ± 44)	151(117)
		2ν	56–92	87%	(53 ± 44)	125(97)
^{142}Ce $\rightarrow$ ^{142}Nd	$2\beta^-$	0ν	1320–1496	84%	$-(26 \pm 36)$	36(15)
		2ν	200–1000	85%	$-(92 \pm 158)$	176(80)

gives the right scale of the experimental sensitivity. Then, a suitable refined determination of the experimental limit is performed.

3.1. Double β processes in ^{136}Ce

As already mentioned above, ^{136}Ce can decay through $2\beta^+$, $\varepsilon\beta^+$ and 2ε. The used $CeCl_3$ crystal contains $N_{136} = 3.12 \times 10^{19}$ ^{136}Ce nuclei. The physics for ^{136}Ce is rather rich. Two positrons could be emitted in its $2\beta^+$ decay with energy up to 375 keV; thus, only the ground state of ^{136}Ba can be populated. The annihilation of these positrons will give rise to four γ's of 511 keV. In the $\varepsilon\beta^+$ decay, not only the ground state but also the first excited level of ^{136}Ba at 818.5 keV can be populated. Finally, in the 2ε capture, many excited 0^+ and 2^+ levels of ^{136}Ba can be populated with the subsequent emission of different γ quanta in the de-excitation process.

The experimental sensitivity to the $2\nu2\beta^+$ decay mode has preliminarily been determined by the 1σ approach. In this case one gets $S/\eta \leqslant 422$ events in the energy interval 596–840 keV, which is the energy interval of interest for the decay mode (see figure 5); this gives a sensitivity: $T_{1/2}^{2\nu2\beta^+} \geqslant 9.6 \times 10^{15}$ yr (68% C.L.). Then, a refined analysis is made: the energy distribution is fitted in the energy range 596–840 keV by the background model, which takes into account the measured residual contaminations, and the expected signal behaviour as evaluated by EGSnrc code. A $\chi^2/n.d.f. = 60.0/60 = 1.00$ is obtained (see figure 5). This approach gives a total number of events, which could be ascribed to the $2\nu2\beta^+$ decay: $S/\eta = -(197 \pm 393)$ counts. This corresponds (in accordance with the Feldman–Cousins procedure [22]) to $\lim S/\eta = 465(221)$ counts at 90%(68%) C.L., giving for the considered process the half-life limit:

$$T_{1/2}^{2\nu2\beta^+}(^{136}\text{Ce}) \geqslant 0.87(1.83) \times 10^{16}\,\text{yr} \quad 90\%(68\%)\,\text{C.L.}$$

In the case of the $0\nu2\beta^+$ decay mode the maximum sensitivity has been obtained in the energy region around 375 keV. The 1σ approach in the energy interval 366–384 keV gives $S/\eta \leqslant 93$ events which corresponds to $T_{1/2}^{0\nu2\beta^+} \geqslant 4.4 \times 10^{16}$ yr (68% C.L.). Then, the experimental data in the 320–436 keV energy interval have been fitted following the same procedure described above, obtaining a $\chi^2/n.d.f. = 38.1/28 = 1.36$ (see figure 5). The total number of events which could be ascribed to the $0\nu2\beta^+$ decay is $S/\eta = -(99 \pm 81)$

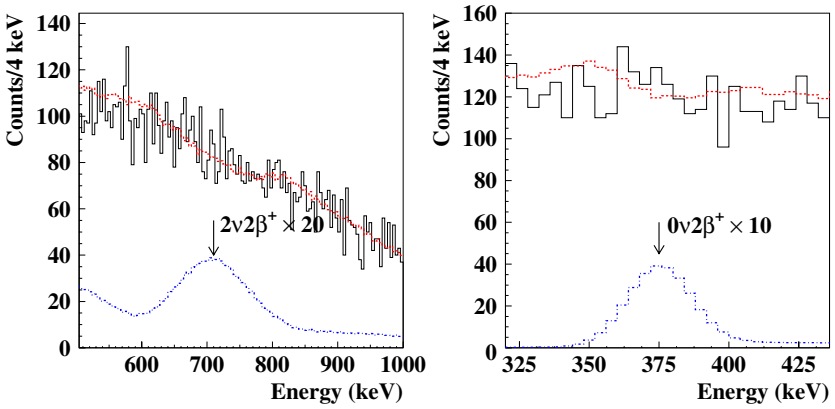

Figure 5. Left: energy distribution around 698 keV where the signal from the $2\nu2\beta^+$ decay mode of ^{136}Ce following the detection of the two positrons and of one of the four γ's emitted in the annihilation process is expected. The dashed line (red) shows the best-fit curve and the histogram presents the experimental data; there is also shown (in dot-dashed blue) the obtained 90% C.L. limit multiplied by a factor 20. (Right) Energy distribution around 375 keV where the signal is expected from the $0\nu2\beta^+$ decay mode of ^{136}Ce when the annihilation γ's escape the detector. The dashed line (red) shows the best-fit curve and the histogram presents the experimental data; there is also shown (in dot-dashed blue) the obtained 90% C.L. limit multiplied by a factor 10.

counts which corresponds to $\lim S/\eta = 55(16)$ counts at 90%(68%) C.L. Thus, the following half-life limit is obtained:

$$T_{1/2}^{0\nu2\beta^+}(^{136}\mathrm{Ce}) \geqslant 0.74(2.53) \times 10^{17}\ \mathrm{yr} \quad 90\%(68\%)\ \mathrm{C.L.}$$

In the $\varepsilon\beta^+$ decay, various particles are emitted: positrons, x-rays and Auger electrons from de-excitations in atomic shells, and γ quanta and/or conversion electrons from de-excitation of a daughter nucleus and from positron annihilation.

The maximum sensitivity to study the $2\nu\varepsilon\beta^+$ decay is obtained in the energy interval 200–1000 keV (see figure 6). The 1σ approach in this energy interval gives: $S/\eta \leqslant 164$ events, and $T_{1/2}^{2\nu\varepsilon\beta^+} \geqslant 2.5 \times 10^{16}$ yr (68% C.L.). Then, the energy spectrum has been fitted in the same energy range according to the aforementioned procedure, obtaining a $\chi^2/n.d.f. = 257/199 = 1.29$ (see figure 6). The total number of events which could be ascribed to the $2\nu\varepsilon\beta^+$ decay mode is $S/\eta = -(102 \pm 160)$ counts which corresponds to $\lim S/\eta = 171(75)$ counts at 90%(68%) C.L. and, thus, to

$$T_{1/2}^{2\nu\varepsilon\beta^+}(^{136}Ce) \geqslant 2.4(5.4) \times 10^{16}\ \mathrm{yr} \quad 90\%(68\%)\ \mathrm{C.L.}$$

For the $0\nu\varepsilon\beta^+$ decay, the 1σ approach was applied in the energy interval 1371–1423 keV ($\pm 1\ \sigma$ around the expected signal peak at 1397 keV); however, in this case the tail of the nearby composite background structure affect this estimate. Anyhow, in this way we obtain $S/\eta \leqslant 26$ events, which corresponds to $T_{1/2}^{0\nu\varepsilon\beta^+} \geqslant 1.6 \times 10^{17}$ yr (68% C.L.). Then, the energy spectrum was fitted in the energy range 1328–1504 keV following the aforementioned procedure, obtaining a $\chi^2/n.d.f. = 17.1/21 = 0.81$ (see figure 6). The total number of events which could be ascribed to the $0\nu\varepsilon\beta^+$ decay mode is $S/\eta = -(53 \pm 55)$ counts; this corresponds to $\lim S/\eta = 46(16)$ counts at 90%(68%) C.L., and to

$$T_{1/2}^{0\nu\varepsilon\beta^+}(^{136}\mathrm{Ce}) \geqslant 0.88(2.53) \times 10^{17}\ \mathrm{yr} \quad 90\%(68\%)\ \mathrm{C.L.}$$

As regards the case of 2ε decay, we have studied just the case of the double electron capture from K shell (binding energy: 37.44 keV). In particular, the $2\nu2K$ gives a structure

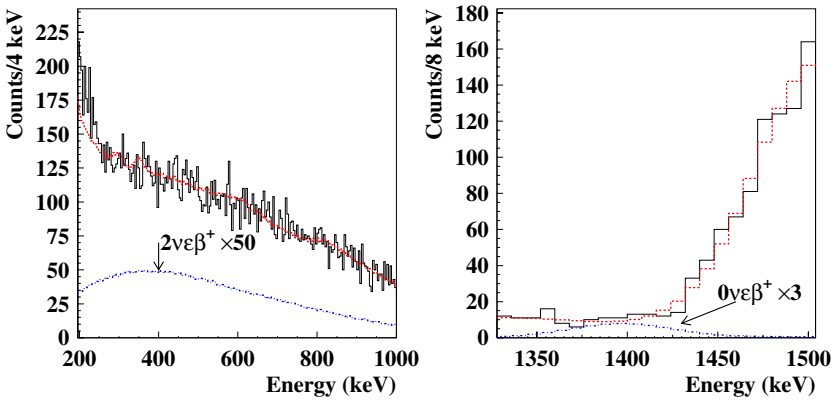

Figure 6. Left: energy distribution in the 200–1000 keV energy interval where the signal is expected from the $2\nu\varepsilon\beta^+$ decay mode of ^{136}Ce following the detection of one positron and of the x-rays and Auger electrons. The dashed line (red) shows the best-fit curve and the histogram presents the experimental data; there is also shown (in dot-dashed blue) the obtained 90% C.L. limit multiplied by a factor of 50. Right: energy distribution around 1397 keV where the signal is expected from the $0\nu\varepsilon\beta^+$ decay mode of ^{136}Ce when the annihilation photons escape the detector. The dashed line (red) shows the best-fit curve and the histogram presents the experimental data; there is also shown (in dot-dashed blue) the obtained 90% C.L. limit multiplied by a factor 3.

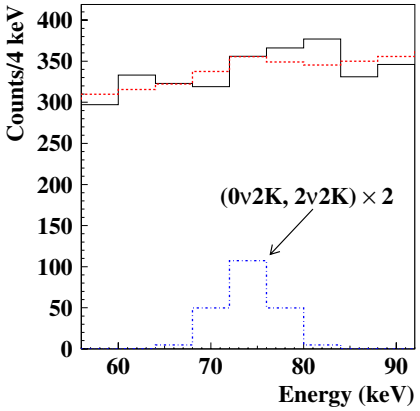

Figure 7. Energy distribution around 75 keV where the signal from the $2\nu 2K$ decay mode of ^{136}Ce following the detection of the x-rays and Auger electrons as well as the signal from the $0\nu 2K$ decay mode is expected . The horizontal dashed line (red) shows the best-fit curve and the histogram presents the experimental data; there is also shown in dot-dashed (blue) line the obtained 90% C.L. limit multiplied by 2 on the $2\nu 2K$ and on $0\nu 2K$ decay modes (both for ^{136}Ce and ^{138}Ce).

around $\simeq$75 keV (sum of the binding energies of the two electrons from the K shell). The 1σ approach in the energy range 72–78 keV ($\pm 1\ \sigma$ around the expected signal peak) gives $S/\eta \leqslant 39$ events which corresponds to $T_{1/2}^{2\nu 2K} \geqslant 1.0 \times 10^{17}$ yr (68% C.L.). Then, the energy spectrum was fitted in the energy range 56–92 keV by the background model (here—due to the small energy window and the quite smooth energy spectrum—it is assumed as a straight line) and the signal simulated with EGSnrc code (see figure 7); a $\chi^2/n.d.f. = 7.4/6 = 1.2$ is obtained. The total number of events which could be ascribed to the $2\nu 2K$ decay mode is

$S/\eta = (53 \pm 44)$ counts which corresponds to lim $S/\eta = 125(97)$ counts at 90%(68%) C.L., and to

$$T_{1/2}^{2\nu 2K}(^{136}\mathrm{Ce}) \geqslant 3.2(4.2) \times 10^{16}\,\mathrm{yr} \quad 90\%(68\%)\,\mathrm{C.L.}$$

In the $0\nu 2\varepsilon$ process, in addition to the particles described above some other particle(s) should be emitted to take away the energy released instead by the two neutrinos in the $2\nu 2\varepsilon$ process. Usually a (bremsstrahlung) gamma quantum is assumed, and in the following we also suppose de-excitation by one γ quantum. Its energy will be equal to $E_\gamma = Q - E_{b1} - E_{b2}$, where E_{b1} and E_{b2} are the binding energies of the first and of the second captured electron on the corresponding atomic shells. For ^{136}Ce, this bremsstrahlung gamma quantum will have energy at least of 2344 keV. In the present experimental set-up the low mass of the used $CeCl_3$ crystal gives a very low peak efficiency for the detection of this gamma quantum of the order of 0.01%, which makes its detection very difficult. However, the $0\nu 2K$ can also be identified by the peak at $\simeq 75$ keV, taking into account the different detection efficiency with the respect to the $2\nu 2K$ process. In particular, rescaling by efficiencies the result of the previous fit we obtain for the $0\nu 2K$ decay mode: $S/\eta = (58 \pm 48)$ counts; this corresponds to lim $S/\eta = 137(106)$ counts at 90%(68%) C.L. and to

$$T_{1/2}^{0\nu 2K}(^{136}\mathrm{Ce}) \geqslant 3.0(3.8) \times 10^{16}\,\mathrm{yr} \quad 90\%(68\%)\,\mathrm{C.L.}$$

3.2. Double electron capture in ^{138}Ce

As already mentioned in the introduction, the ^{138}Ce isotope can decay only through 2ε with $Q = 693(10)$ keV. Its natural abundance is $\delta = 0.251\%$; thus, the used $CeCl_3$ crystal contains $N_{138} = 4.23 \times 10^{19}$ nuclei.

We have studied the 2ε decay of the ^{138}Ce analysing the case of the K shell electron capture. In fact, the process of relaxation in the atomic shell of ^{138}Ba after the $2\nu 2K$ capture in ^{138}Ce is exactly the same as for ^{136}Ce. Thus, we can use our previous calculations for ^{136}Ce just correcting for the different number of ^{138}Ce nuclei. It gives the following limit:

$$T_{1/2}^{2\nu 2K}(^{138}\mathrm{Ce}) \geqslant 4.4(5.7) \times 10^{16}\,\mathrm{yr} \quad 90\%(68\%)\,\mathrm{C.L.}$$

The $0\nu 2K$ capture in ^{138}Ce is also similar to the $0\nu 2K$ process in ^{136}Ce. However, the energy of the emitted additional γ quantum (618 keV) is lower for ^{138}Ce than for ^{136}Ce (2344 keV). This leads to slightly lower efficiency for the detection of the 75 keV peak. The final values for the $T_{1/2}$ limit are as follows:

$$T_{1/2}^{0\nu 2K}(^{138}\mathrm{Ce}) \geqslant 3.6(4.7) \times 10^{16}\,\mathrm{yr} \quad 90\%(68\%)\,\mathrm{C.L.}$$

3.3. 2β decays of ^{142}Ce

As already mentioned in the introduction, the ^{142}Ce isotope can decay through $2\beta^-$ with $Q = 1416.7$ keV. The natural abundance is $\delta = 11.114\%$; thus the used $CeCl_3$ crystal contains $N_{142} = 1.87 \times 10^{21}$ nuclei.

In the $2\beta^-$ decay the particles emitted are electrons and neutrinos (in the mode 2ν); thus, to detect this process with good efficiency it is needed that the decaying isotope is inside the detector itself as in the present case.

The signal expected for the $2\nu 2\beta^-$ decay mode is continuous with a maximum around 400 keV (see figure 8, left).

The maximum sensitivity to study this decay mode is achieved in the energy interval 200–1000 keV (see figure 8, left). The 1σ approach in this energy interval gives $S/\eta \leqslant 165$

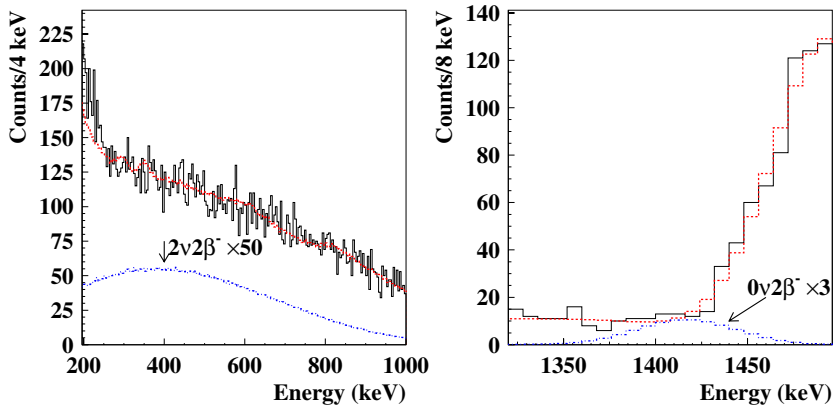

Figure 8. Left: energy distribution in the 200–1000 keV energy interval where the signal from the $2\nu2\beta^-$ decay mode of ^{142}Ce following the detection of the electrons is mainly expected. The dashed line (red) shows the best-fit curve and the histogram presents the experimental data; there is also shown (in dot-dashed blue) the obtained 90% C.L. limit multiplied by a factor 50. Right: energy distribution around 1417 keV where the signal from the $0\nu2\beta^-$ decay mode of ^{142}Ce is expected. The dashed line (red) shows the best-fit curve and the histogram presents the experimental data; there is also shown (in dot-dashed blue) the obtained 90% C.L. limit multiplied by a factor 3.

Table 4. Half-life limits on 2β processes (ground state to ground state transitions) in cerium isotopes at 90%(68%) C.L. Theoretical values for 0ν mode are given for the effective neutrino mass of 1 eV. More theoretical results can be found in compilations [2].

Transition	Decay channel	Decay mode	Exp. $T_{1/2}$ limit (yr)		Theoretical
			Present work	Previous results	$T_{1/2}$ (yr)
^{136}Ce $\rightarrow$ ^{136}Ba	$2\beta^+$	0ν	$> 0.7(2.5) \times 10^{17}$	$> (6.9) \times 10^{17}$ [9]	2.4×10^{29} [6]
					2.7×10^{29} [23]
		2ν	$> 0.9(1.8) \times 10^{16}$	$> 1.8 \times 10^{16}$ [10]	5.2×10^{31} [6]
	$\varepsilon\beta^+$	0ν	$> 0.9(2.5) \times 10^{17}$	$> 3.8 \times 10^{16}$ [10]	4.7×10^{26} [6]
					4.0×10^{26} [23]
		2ν	$> 2.4(5.4) \times 10^{16}$	$> 2.6 \times 10^{15}$ [11]	9.2×10^{23} [6]
					6.0×10^{23} [24]
	$2K$	0ν	$> 3.0(3.8) \times 10^{16}$	$> 6.0 \times 10^{15}$ [10]	–
		2ν	$> 3.2(4.2) \times 10^{16}$	$> 2.7 \times 10^{16}$ [8]	3.2×10^{18}–6.4×10^{19} [25]
					$(3.2–5.1) \times 10^{21}$ [26]
					9.6×10^{21} [24]
^{138}Ce $\rightarrow$ ^{138}Ba	$2K$	0ν	$> 3.6(4.7) \times 10^{16}$	$> 1.9 \times 10^{15}$ [11]	–
		2ν	$> 4.4(5.7) \times 10^{16}$	$> 3.7 \times 10^{16}$ [8]	$\geqslant 2.1 \times 10^{26}$ [27]
^{142}Ce $\rightarrow$ ^{142}Nd	$2\beta^-$	0ν	$> 0.7(1.6) \times 10^{19}$	$> (1.5) \times 10^{19}$ [9]	2.8×10^{24} [28]
		2ν	$> 1.4(3.0) \times 10^{18}$	$> 1.6 \times 10^{17}$ [10]	2.2×10^{20}–4.2×10^{21} [28]
					2.3×10^{23} [29]

events, and $T_{1/2}^{2\nu2\beta^-} \geqslant 1.5 \times 10^{18}$ yr (68% C.L.). Then, the energy spectrum has been fitted in the same energy range by the background model and by the $2\beta^-$ signal simulated with

EGSnrc code, obtaining a $\chi^2/n.d.f. = 257/199 = 1.28$ (see figure 8, left). The total number of events which could be ascribed to the $2\nu2\beta^-$ decay mode is $S/\eta = -(92 \pm 158)$ counts which corresponds to $\lim S/\eta = 176(80)$ counts at 90%(68%) C.L. and, thus, to

$$T_{1/2}^{2\nu2\beta^-}(^{142}\mathrm{Ce}) \geqslant 1.4(3.0) \times 10^{18}\,\mathrm{yr} \quad 90\%(68\%)\,\mathrm{C.L.}$$

For the $0\nu2\beta^-$ decay, the 1σ approach was applied in the energy interval 1391–1443 keV ($\pm$ 1 σ around the expected signal peak at 1417 keV); however, in this case the tail of the nearby composite background structure affects this estimate. Anyhow, in this way we obtain $S/\eta \leqslant 19$ events, which corresponds to $T_{1/2}^{0\nu2\beta^-} \geqslant 1.3 \times 10^{19}$ yr (68% C.L.). Then, the energy spectrum was fitted in the energy range 1320–1496 keV by the background model and the signal simulated with EGSnrc code, obtaining a $\chi^2/n.d.f. = 15.3/21 = 0.73$ (see figure 8, right). The total number of events which could be ascribed to the $0\nu2\beta^-$ decay mode is $S/\eta = -(26 \pm 36)$ counts; this corresponds to $\lim S/\eta = 36(15)$ counts at 90%(68%) C.L., and to:

$$T_{1/2}^{0\nu2\beta^-}(^{142}\mathrm{Ce}) \geqslant 0.67(1.62) \times 10^{19}\,\mathrm{yr} \quad 90\%(68\%)\,\mathrm{C.L.}$$

4. Conclusions

A search for double beta processes in cerium isotopes has been realized by using for the first time a small $CeCl_3$ crystal scintillator to realize the 'source = detector' approach. In spite of the small exposed mass (6.9 g) and of the limited time of measurements (1638 h) some new improved half-life limits have been obtained as summarized in table 4, where also the results of the previous most sensitive experiments are given for comparison.

This supports the interest in realizing larger mass and longer exposure deep underground with new $CeCl_3$ crystal scintillators exploiting the active source technique. A further relevant topic is the future preliminary selection of all the materials and of the growing/handling procedures as well as the development of chemical/physical purification techniques in order to improve the radiopurity of the crystal and housing materials. In particular, the ^{138}La contamination could be related mainly to the growing process; in fact, the crystal used here was realized just after the growth of a $LaCl_3$ scintillator. Moreover, the use of a larger TD sampling frequency and of different optical read-out should be considered in order to have the possibility of effectively applying the PSD for internal α background reduction when of interest. In addition, the $2\beta^+$ and $\varepsilon\beta^+$ processes can give strong signature when coincidences with other close detectors are investigated. It should also be stressed the advantage of much better energy resolution of $CeCl_3$ crystal scintillator (FWHM $\approx$ 5% at 662 keV γ line of ^{137}Cs) in comparison with f.e. CeF_3 crystal scintillators ($\approx$ 18% at the same energy) [8].

Further improvements in sensitivity can be reached by using enriched ^{136}Ce, increasing the detection efficiency by using larger $CeCl_3$ detector, and developing $CeCl_3$ scintillators with lower level of radioactive contamination. An experiment involving $\approx$100 kg of crystals enriched in ^{136}Ce to 20% (5×10^{25} nuclei of ^{136}Ce) could reach over 5 years of measurements the half-life sensitivity $T_{1/2} \approx 10^{25}$ yr (supposing zero background). Such a sensitivity could contribute to our understanding of the neutrino mass mechanism and right-handed currents in neutrinoless processes [6]. Particular interest is offered by the $2\nu2\varepsilon$ decay mode of ^{136}Ce, whose half-life is expected to be in the range 10^{18}–10^{22} yr by theoretical estimates [2]; thus, this process should be observed in such an experiment.

Acknowledgment

The authors would like to express gratitude to the referees for their careful reading of the manuscript and their useful comments.

References

[1] Avignone F T III, Elliott S R and Engel J 2008 *Rev. Mod. Phys.* **80** 481
Klapdor-Kleingrothaus H V 2008 *Int. J. Mod. Phys.* E **17** 505
Ejiri H 2005 *J. Phys. Soc. Japan* **74** 2101
Avignone F T III, King G S and Zdesenko Yu G 2005 *New J. Phys.* **7** 6
Elliot S R and Engel J 2004 *J. Phys. G: Nucl. Part. Phys.* **30** R183
Vergados J D 2002 *Phys. Rep.* **361** 1
Elliot S R and Vogel P 2002 *Ann. Rev. Nucl. Part. Sci.* **52** 115
Zdesenko Yu G 2002 *Rev. Mod. Phys.* **74** 663
[2] Tretyak V I and Zdesenko Yu G 1995 *At. Data Nucl. Data Tables* **61** 43
Tretyak V I and Zdesenko Yu G 2002 *At. Data Nucl. Data Tables* **80** 83
[3] Barabash A S 2010 *Phys. Rev.* C **81** 035501
[4] Gavriljuk Ju M *et al* 2006 *Phys. At. Nucl.* **69** 2124
Barabash A S *et al* 2007 *J. Phys. G: Nucl. Part. Phys.* **34** 1721
Barabash A S *et al* 2007 *Nucl. Phys.* A **785** 371
Kim H J *et al* 2007 *Nucl. Phys.* A **793** 171
Barabash A S *et al* 2008 *Nucl. Phys.* A **807** 269
Dawson J *et al* 2008 *Nucl. Phys.* A **799** 167
Barabash A S *et al* 2009 *Phys. Rev.* C **80** 035501
Belli P *et al* 2009 *Eur. Phys. J.* A **42** 171
Rukhadze N I *et al* 2010 *J. Phys.: Conf. Ser.* **203** 012072
[5] Belli P *et al* 2008 *Phys. Lett.* B **658** 193
Belli P *et al* 2008 *Eur. Phys. J.* A **36** 167
Belli P *et al* 2009 *Nucl. Phys.* A **826** 256
[6] Hirsch M *et al* 1994 *Z. Phys.* A **347** 151
[7] Barabash A S 2010 *Phys. At. Nucl.* **73** 162
[8] Belli P *et al* 2003 *Nucl. Instrum. Methods* A **498** 352
[9] Bernabei R *et al* 1997 *Nuovo Cimento* A **110** 189
[10] Danevich F A *et al* 2001 *Nucl. Phys.* A **694** 375
[11] Belli P *et al* 2009 *Nucl. Phys.* A **824** 101
[12] Audi G, Wapstra A H and Thibault C 2003 *Nucl. Phys.* A **729** 337
[13] Bohlke J K *et al* 2005 *J. Phys. Chem. Ref. Data* **34** 57
[14] Eijk C W E van 2001 *Nucl. Instrum. Methods* A **460** 1
[15] Kramer K W, Dorenbos P, Gudela H U and van Eijk C W E 2006 *J. Mater. Chem.* **16** 2773
[16] Cappella F *et al* 2010 *Nucl. Instrum. Methods* A **618** 168
[17] Belli P *et al* 2007 *Phys. Rev.* C **76** 064603
Belli P *et al* 2007 *Nucl. Phys.* A **789** 15
Bernabei R *et al* 2006 *Ukr. J. Phys.* **51** 1037
Bernabei R *et al* 2005 *Nucl. Instrum. Methods* A **555** 270
Cerulli R *et al* 2004 *Nucl. Instrum. Methods* A **525** 535
Belli P *et al* 2003 *Nucl. Instrum. Methods* A **498** 352
Bernabei R *et al* 2002 *Nucl. Phys.* A **705** 29
Belli P *et al* 1999 *Nucl. Phys.* B **563** 97
Belli P *et al* 1999 *Astropart. Phys.* **10** 115
Bernabei R *et al* 1997 *Nuovo Cimento* A **110** 189
Bernabei R *et al* 1997 *Astropart. Phys.* **7** 73
[18] Gatti E and de Martini F 1962 *Nuclear Electronics* vol 2 (IAEA, Vienna) p 265
[19] Barnett R M *et al* 1996 *Phys. Rev.* D **54** 159
[20] Kawrakow I and Rogers D W O 2003 The EGS code system *NRCC Report PIRS-701*
[21] Ponkratenko O A *et al* 2000 *Phys. At. Nucl.* **63** 1282
Tretyak V I To be published

[22] Feldman G J and Cousins R D 1998 *Phys. Rev.* D **57** 3873
[23] Suhonen J and Aunola M 2003 *Nucl. Phys.* A **723** 271
[24] Rumyantsev O A and Urin M H 1998 *Phys. Lett.* B **443** 51
[25] Suhonen J 1993 *Phys. Rev.* C **48** 574
[26] Civitarese O and Suhonen J 1998 *Phys. Rev.* C **58** 1535
[27] Abad J *et al* 1984 *J. Physique* **45** C3–147
[28] Staudt A, Muto K and Klapdor-Kleingrothaus H V 1990 *Europhys. Lett.* **13** 31
[29] Bobyk A *et al* 2004 *Eur. Phys. J.* A **19** 327